Hindawi
International Journal of Chemical Engineering
Volume 2018, Article ID 1706405, 8 pages
https://doi.org/10.1155/2018/1706405

Research Article

CO_2 Adsorption from Biogas Using Amine-Functionalized MgO

Preecha Kasikamphaiboon and Uraiwan Khunjan

Department of Science, Faculty of Science and Technology, Prince of Songkla University, Pattani Campus, Pattani 94000, Thailand

Correspondence should be addressed to Preecha Kasikamphaiboon; preecha.kas@psu.ac.th

Received 17 August 2018; Revised 18 November 2018; Accepted 29 November 2018; Published 13 December 2018

Academic Editor: Bhaskar Kulkarni

Biogas is a renewable fuel source of methane (CH_4), and its utilization as a natural gas substitute or transport fuel has received much interest. However, apart from CH_4, biogas also contains carbon dioxide (CO_2) which is noncombustible, thus reducing the biogas heating value. Therefore, upgrading biogas by removing CO_2 is needed for most biogas applications. In this study, an amine-functionalized adsorbent for CO_2 capture from biogas was developed. Mesoporous MgO was synthesized and functionalized with different tetraethylenepentamine (TEPA) loadings by wet impregnation technique. The prepared adsorbents (MgO-TEPA) were characterized by X-ray diffraction (XRD) and N_2 adsorption-desorption. The CO_2 adsorption performance of the prepared MgO-TEPA was tested using simulated biogas as feed gas stream. The results show that the CO_2 adsorption capacities of the adsorbents increase with increasing TEPA loading. The optimum TEPA loading is 40 wt.%, which gives the highest CO_2 adsorption capacity of 4.98 mmol/g. A further increase in TEPA loading to 50 wt.% significantly reduces the CO_2 adsorption capacity. Furthermore, the stability and regenerability of the adsorbent with 40% TEPA loading (MgO-TEPA-40) were studied by performing ten adsorption-desorption cycles under simulated biogas and real biogas conditions. After ten adsorption-desorption cycles, MgO-TEPA-40 shows slight decreases of only 5.42 and 5.75% of CO_2 adsorption capacity for the simulated biogas and biogas, respectively. The results demonstrate that MgO-TEPA-40 possesses good stability and regenerability which are important for the potential application of this amine-based adsorbent.

1. Introduction

Due to rising fossil fuel prices, greenhouse gas emissions from fossil fuel combustion, and high energy demands, sustainable and renewable energy sources are needed [1, 2]. Biogas, considered to be one of the alternative sources of renewable energy, has the potential to supplement the current energy requirements. Biogas produced from anaerobic digestion processes is mainly composed of 50–70% of methane (CH_4) and 30–50% of carbon dioxide (CO_2) [3]. Apart from these two gases, biogas contains smaller amounts of hydrogen sulfide (H_2S) and trace amounts of ammonia (NH_3), nitrogen (N_2), hydrogen (H_2), carbon monoxide (CO), and oxygen (O_2) [4, 5]. The energy content in terms of calorific value of pure methane is 36 MJ/m^3 (at STP conditions), whereas that of the biogas containing 60–65% CH_4 is approximately 20–25 MJ/m^3 [3, 6]. Therefore, being noncombustible, CO_2 also causes a reduction in the heating value and energy density of biogas on volume basis. In addition, high CO_2 content increases energy demand for compression and transportation of biogas. Biogas can be upgraded to a higher fuel standard by increasing the energy density by reducing major noncombustible gas (CO_2) and other impurities. The final product consisting of 95–99% CH_4 and 1–5% CO_2 [7], which is called biomethane, can be used as a substitute for natural gas and a vehicle fuel. Therefore, upgrading biogas to biomethane is one of the technologies that receive much attention in the bioenergy industry.

To remove acid gases such as CO_2 and H_2S from gas streams, several technologies have been developed, including physical absorption, chemical absorption, adsorption, membrane separation, and cryogenic separation [8]. Among these technologies, the chemical absorption using liquid amine absorbents is one of the most widely used technologies for separating CO_2 from gas streams [9, 10]. However, amine scrubbing processes have some disadvantages such as high energy consumption for solvent regeneration, high equipment corrosion rate, solvent degradation, and fouling of the

process equipment [11–13]. As a result, adsorption-based technologies, usually involving solid CO_2 adsorbents, are suggested and studied to overcome those problems [14]. Adsorbents for CO_2 capture are mainly porous materials, such as activated carbon [15, 16], mesoporous silica [17], zeolites [18, 19], and metal-organic frameworks (MOFs) [20, 21], which usually have a large surface area in mesopores and micropores. Compared to liquid amine absorption, the solid adsorbents possess significant advantages for energy efficiency. However, there are some existing problems such as low CO_2 adsorption capacities and selectivity. Therefore, modification or functionalization of the solid adsorbents by introducing amines into their porous structure for CO_2 adsorption has also attracted great interest [22]. The amine-functionalized adsorbents combine the high CO_2 affinity of amines and porous materials (large pore volume and large surface area) which exhibit advantageous properties such as high CO_2 adsorption rate and high thermal stability. These adsorbents not only have the potential to reduce the energy consumption compared to the large amount of energy required to heat bulk water for the regeneration of absorbent in the aqueous amine absorbent process but also have high CO_2 adsorption capacity and the ability to reduce the corrosion of equipment caused by high concentrated aqueous amine absorbent [10, 23]. Several research groups have studied and reported the performances of mesoporous materials functionalized with amines for CO_2 removal. These materials can be grouped together depending on the preparation methods which are grafting and impregnation with diverse amine species such as aminosilanes, polyethylenimine (PEI), tetraethylenepentamine (TEPA), and diethanolamine (DEA) [24–31]. The adsorbents obtained by chemical grafting of amine onto the support are relatively more stable than those obtained by physical impregnation. However, the amount of grafted amine is limited, resulting in a relatively lower amine loading which leads to lower CO_2 adsorption capacity. Unlike the grafting method, the impregnation method possesses several advantages such as easier preparation, higher amine loading, and lower cost [32].

Apart from the solid adsorbents mentioned above, magnesium oxide (MgO) has been widely studied for CO_2 capture and has been reported as a potential adsorbent for CO_2 adsorption [33–35]. However, pure MgO exhibits fairly small CO_2 adsorption capacity [36]. To the best of our knowledge, introducing amines into the porous structure of MgO to form a composite with high CO_2 adsorption capacity has not been reported. Therefore, in the present study, a new adsorbent for CO_2 removal from biogas was developed. MgO with mesoporous structure was synthesized and functionalized with tetraethylenepentamine (TEPA) via an impregnation process. The prepared adsorbents with different amine loadings were investigated for CO_2 adsorption capacity. Multiple adsorption-desorption cyclic stability of the adsorbents was also tested by using simulated biogas and biogas as feed gas streams.

2. Experimental

2.1. Synthesis of Mesoporous MgO. Mesoporous MgO was synthesized using the sol-gel method as reported in the literature [37]. Magnesium nitrate hexahydrate ($Mg(NO_3)_2 \cdot 6H_2O$) and oxalic acid ($(COOH)_2 \cdot 2H_2O$), purchased from Sigma-Aldrich, in the molar ratio of 1 : 1, were first dissolved separately in ethanol and used for the synthesis of MgO. These solutions were then mixed together with vigorous magnetic stirring to yield a thick white gel and kept stirred for 12 h. Subsequently, the gel product was dried at 100°C for 24 h. The dried mixture was ground and calcined under atmospheric pressure at 600°C for 2 h. The chemical reactions in the sol-gel and calcination step can be expressed by equations (1) and (2), respectively [37]:

$$\begin{aligned} &Mg(NO_3)_2 \cdot 6H_2O + (COOH)_2 \cdot 2H_2O \\ &\longrightarrow MgC_2O_4 \cdot 2H_2O + 2HNO_3 + 6H_2O \end{aligned} \quad (1)$$

$$MgC_2O_4 \cdot 2H_2O + 0.5O_2 \longrightarrow MgO + 2CO_2 + 2H_2O \quad (2)$$

2.2. Preparation of Amine-Functionalized Adsorbents. In this study, the amine-functionalized adsorbents were prepared by the wet impregnation method described by Xu et al. [38] with some modification. The desired amount of tetraethylenepentamine (TEPA), obtained from Sigma-Aldrich, was dissolved in 25 ml of methanol under stirring for 15 min. Then, 5 g of the synthesized MgO was added to the TEPA-methanol solution, and the resultant slurry was stirred continuously for approximately 30 min. The slurry was then dried at 70°C for 2 h. The adsorbents impregnated with TEPA were designated as MgO-TEPA-x, where x represents the weight percentage of TEPA in the adsorbents.

2.3. Characterization of the Adsorbents. The crystal structures of the prepared adsorbents were analyzed by powder X-ray diffraction (PXRD) by using a Philips X'Pert MPD diffractometer with Cu-Kα radiation. The N_2 adsorption-desorption isotherms were measured at −196°C using a Micromeritics ASAP2060 volumetric analyzer. The isotherms were used for calculating the surface area, pore volume, and average pore diameter of the adsorbents via the Brunauer–Emmett–Teller (BET) method and the Barrett–Joyner–Halenda (BJH) method.

2.4. CO_2 Adsorption. The CO_2 adsorption-desorption tests were performed in a fixed-bed reactor of which a simplified flow diagram is given in Figure 1. The reactor was a stainless-steel adsorption column with an inner diameter of 15 mm and a length of 160 mm. Typically, 5 g of the adsorbent was packed into the adsorption column and supported by quartz wool from both sides. Before each experimental run, the sample was heated to 100°C in a N_2 (99.99% purity) stream at the flow rate of 40 mL/min for 60 min. After cooling to the adsorption temperature (30°C), the adsorption tests began by introducing simulated biogas into the adsorption column at a flow rate of 40 mL/min. The simulated biogas was produced by mixing CO_2 (99.99% purity) and N_2 (99.99% purity) from gas cylinders at the desired flow rates to obtain a concentration of 40% CO_2 and 60% N_2. The adsorbent-bed

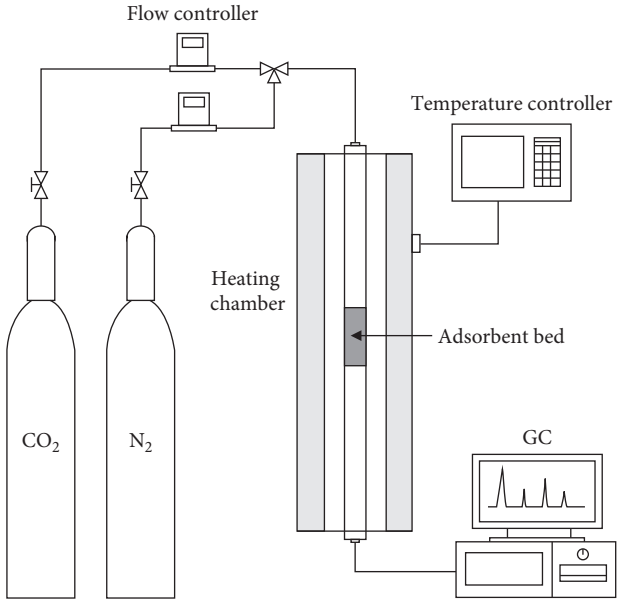

Figure 1: Schematic diagram of the CO_2 adsorption system.

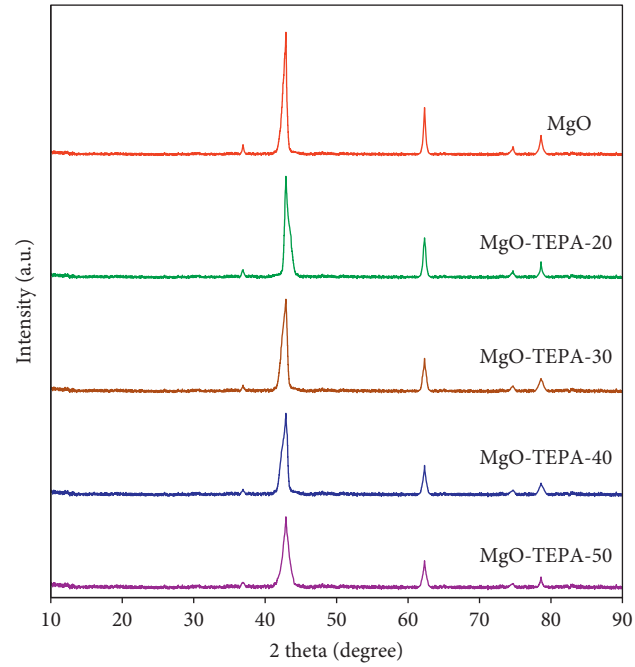

Figure 2: XRD patterns of MgO with different TEPA loadings.

temperature was measured by thermocouples and controlled by a temperature controller. After completing the adsorption process, desorption of the adsorbed CO_2 was performed by heating the sample to 150°C in a N_2 gas stream for 60 min. In order to test the regenerability of the adsorbent, ten cycles of adsorption-desorption were performed on the same sample. In this study, biogas produced from a local swine farm was also used as feed gas to test the CO_2 adsorption performance of the prepared adsorbent using the same experimental procedure. The biogas consists of 38.4% CO_2 and 61.5% CH_4, which are in the range of the typical biogas compositions found in the literature [39]. The concentrations of CO_2 in the feed and treated gas streams were determined by a gas chromatograph equipped with a TCD detector.

The breakthrough curve data obtained from the CO_2 adsorption tests were used for calculating the equilibrium capacity of the adsorbents according to equations (3) and (4) [40]:

$$q = \frac{Qt_sC_0}{22.4m}, \tag{3}$$

$$t_s = \int_0^t \left(1 - \frac{C_t}{C_0}\right) dt, \tag{4}$$

where t_s is the mean residence time (min), C_0 and C_t are the inlet and outlet concentrations of CO_2 (vol.%), respectively, q is the equilibrium adsorption capacity of CO_2 (mmol/g), t is the adsorption time (min), Q is the feed volumetric flow rate (ml/min) at standard temperature and pressure (STP), and m is the mass of the adsorbent (g).

3. Results and Discussion

3.1. Characterization. Figure 2 shows the XRD patterns of the prepared MgO with different TEPA loadings. The pristine MgO exhibits five well-resolved diffraction peaks at 36.9°, 42.9°, 62.3°, 74.7°, and 78.6°. These are characteristic peaks of MgO, which are consistent with the results of previous reports [35, 41, 42]. This confirms a high degree of purity and suggests that the obtained MgO samples are highly crystalline. From comparing the diffraction pattern of MgO with those of MgO-TEPA-x with different TEPA loadings; the diffraction angles are nearly identical, indicating that the structure of MgO is preserved after loading the TEPA. However, the diffraction intensity of MgO decreases with increasing TEPA loadings. It has been reported that diffraction intensities are relative to the degrees of pore filling [43]. Therefore, the incorporation of amine into the pore channels of the support possibly causes the loss of intensity [28]. This indicates that TEPA is loaded into the pore of the MgO support, which is similar to that observed in MCM-41 loaded with polyethylenimine (PEI) [38].

To investigate the porous structure of the prepared samples, N_2 adsorption-desorption isotherms were measured. Figure 3 shows the N_2 adsorption-desorption isotherms of the prepared MgO with different TEPA loadings. According to the International Union of Pure and Applied Chemistry (IUPAC) classification [44], all of the samples display type IV isotherms with the hysteresis loop. The hysteresis loop present in the isotherm is due to the capillary condensation taking place in mesopores. The pristine MgO exhibits a large hysteresis loop compared with the other four TEPA-functionalized samples, indicating the presence of highly porous structure. In addition, it can be seen that the N_2 uptake decreases with increasing TEPA loading. As the TEPA loading increases from 20 to 50 wt.%, the mesopores of MgO are almost completely filled with TEPA molecules at 50 wt.% which results in restricting the access of N_2 into the pores, thus causing MgO-TEPA-50 to become a nonporous material [45].

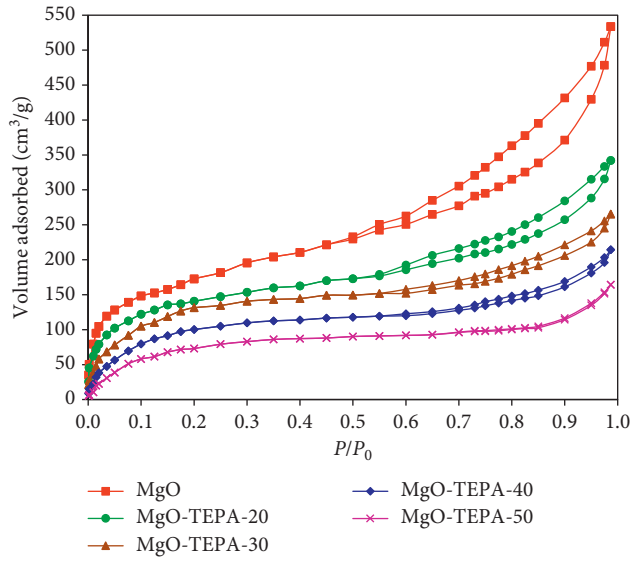

Figure 3: Adsorption-desorption isotherms of MgO with different TEPA loadings.

From the N_2 adsorption-desorption isotherms, the surface area, pore volume, and average pore diameter of the MgO samples were calculated according to the BET and BJH method and are listed in Table 1. Loading TEPA onto MgO significantly reduces the surface area and pore volume. For example, when the TEPA loading is 20 wt.%, the surface area and the pore volume decrease from 207 to 118 m^2/g and from 0.81 to 0.53 cm^3/g, respectively. A further increase in TEPA loading to 50 wt.% causes a great decrease in the surface area and the pore volume. This is because, when the TEPA loading reaches 50 wt.% or higher, excessive amount of TEPA blocks most of the pores and covers the surface of the adsorbent [46, 47]. The same trend as the surface area and pore volume is observed for the pore size of the samples.

3.2. CO_2 Adsorption Behaviors. The effect of TEPA loading on the CO_2 adsorption performance of MgO-TEPA was investigated using simulated biogas as the feed gas. Figures 4 and 5 show the breakthrough curves and the adsorption capacities (mmol of CO_2/g of adsorbent), respectively. As can be seen, the CO_2 adsorption of the pristine MgO reaches the saturation point within only 12 min, resulting in a low adsorption capacity of 0.95 mmol/g. Increasing TEPA loading within a suitable range increases the breakthrough time and adsorption capacity of the adsorbents, which is consistent with the results of previous reports [48, 49]. This is because, as the loading increases, more amine active sites for CO_2 adsorption are provided. When the TEPA loading increases to 40 wt.% (MgO-TEPA-40), the adsorbent shows the maximum breakthrough time and adsorption capacity of 34 min and 4.98 mmol/g, respectively. However, as the TEPA loading increases from 40 to 50 wt.%, the breakthrough time and the adsorption capacity significantly drop from 34 to 28 min and from 4.98 to 4.26 mmol/g, respectively. Too high loadings may cause the TEPA molecules to aggregate in the pore or coat the surface of the adsorbent,

Table 1: Surface area, pore volume, and average pore diameter of MgO-TEPA-*x*.

Adsorbent	BET surface area (m^2/g)	Pore volume (cm^3/g)	Pore diameter (nm)
MgO	207	0.81	7.3
MgO-TEPA-20	118	0.53	4.6
MgO-TEPA-30	54	0.39	3.2
MgO-TEPA-40	19	0.22	1.9
MgO-TEPA-50	4	0.08	1.1

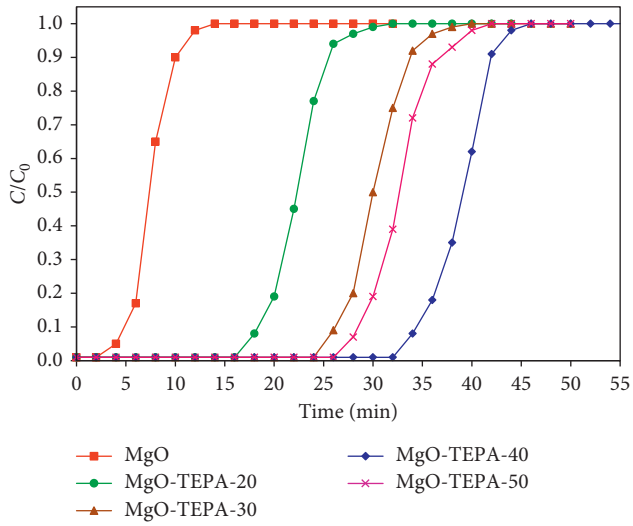

Figure 4: Breakthrough curves of MgO with different TEPA loadings.

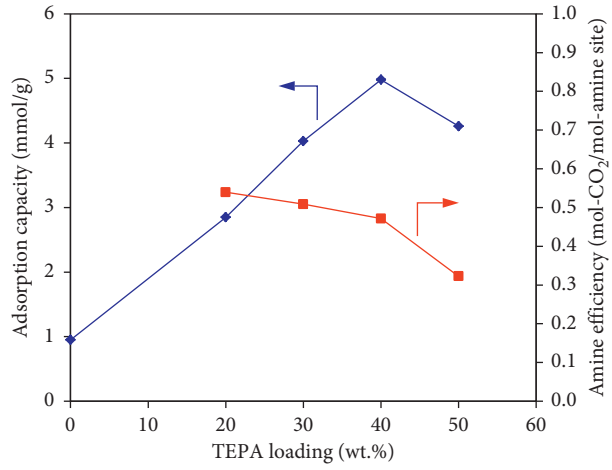

Figure 5: CO_2 adsorption capacity and amine efficiency of MgO with different TEPA loadings.

which hinder the diffusion of CO_2 to react with the active sites in the pores [48, 50]. The above results suggest that the optimum TEPA loading for MgO modification is 40 wt.%.

The most common mechanism for CO_2 capture in supported amines under dry conditions involves the formation of carbamates between two amine groups [51, 52]. Two types of these amine groups exist within TEPA including primary (R_1-NH_2) and secondary (R_1-NH-R_2)

Table 2: Comparison of CO_2 adsorption capacity of amine-impregnated adsorbents.

Support	Amine		Gas composition	Adsorption temperature (°C)	CO_2 adsorption capacity (mmol/g)	Reference
	Type	wt.%				
MCM-41	PEI	75	100% CO_2	75	3.02	[28]
SBA-15	PEI	50	15% CO_2	75	3.18	[53]
Carbon black	PEI	50	100% CO_2	75	3.07	[54]
SBA-15	PEI	50	100% CO_2	75	2.89	[55]
KIT-6	PEI	50	100% CO_2	75	3.07	[55]
KIT-6	PEI	50	100% CO_2	105	3.10	[56]
SBA-15	TEPA	70	100% CO_2	75	3.93	[57]
HMS	PEI	60	100% CO_2	75	4.18	[58]
AC	DETA	39	100% CO_2	25	0.91	[59]
Al_2O_3	DETA	40	100% CO_2	25	1.41	[60]
SiO_2	APTES	70	10% CO_2	100	2.03	[61]
PMMA	PEI	40	15% CO_2	45	3.65	[62]
SBA-15	PEI	60	15% CO_2	75	3.14	[63]
MMSV	PEI	60	100% CO_2	90	4.73	[64]
MSU-J	TEPA	50	100% CO_2	25	3.73	[50]
MgO	—	—	40% CO_2	30	0.95	This study
MgO	TEPA	40	40% CO_2	30	4.98	This study

amines. The reactions of CO_2 with the primary and secondary amines in TEPA can be represented as in equations (5)–(7) [52]:

$$CO_2 + 2R_1NH_2 \longleftrightarrow (R_1NHCOO^-)(R_1NH_3^+) \quad (5)$$

$$CO_2 + 2R_1R_2NH \longleftrightarrow (R_1R_2NCOO^-)(R_1R_2NH_2^+) \quad (6)$$

$$CO_2 + R_1NH_2 + R_1R_2NH \longleftrightarrow (R_1R_2NCOO^-)(R_1NH_3^+) \quad (7)$$

In order to explore the degree of utilization of amine groups in TEPA by CO_2, the amine efficiency was defined as the molar ratio of the adsorbed CO_2 to all amine groups present in the adsorbents [48]. The number of amine groups was calculated from the molar amount of nitrogen atoms in TEPA. The molecular weight of TEPA is 189.3 g/mol, and each TEPA molecule contains 5 amine groups. Therefore, the amine efficiency was calculated and is presented in Figure 5. It can be seen that the amine efficiency decreases with an increase in TEPA loading. The highest amine efficiency of 0.54 is obtained at 20 wt.% TEPA loading, suggesting that two moles of amine groups reacts with one mole of CO_2. At low TEPA loading, the amine chains are more dispersible, making the adsorption sites easily available. However, as the amine loading increases, amines would begin to conglomerate within the pores. This leads to poor distribution of amine sites, resulting in a reduction in the number of the accessible amine sites for CO_2 sorption, although the potential amine sites are more for higher TEPA loading. With a further increase in TEPA loading to 50 wt.%, the amine efficiency decreases significantly to 0.32, indicating that some of amine sites are unoccupied.

The CO_2 adsorption capacities of MgO and MgO-TEPA-40 in this study and those of amine-impregnated adsorbents reported in the literature are compared in Table 2. As can be seen, various supports and amines are used for adsorbent preparation. The comparison shows that the CO_2 adsorption capacity of MgO-TEPA-40 is higher than those previously reported in the literature.

3.3. Regenerability of the Adsorbents. In industrial applications, the stability and regenerability of CO_2 adsorbents are critical parameters for long-term operation. In this study, the cyclic CO_2 adsorption capacity of MgO-TEPA-40 was investigated by performing ten CO_2 adsorption-desorption cycles using simulated biogas and real biogas as feed gas streams. Figure 6 shows the cyclic CO_2 adsorption capacities of the adsorbent in ten consecutive runs. For the simulated biogas, the CO_2 adsorption capacity decreases slightly with increasing number of adsorption-desorption cycle. After ten cycles, the CO_2 adsorption capacity decreases from 4.98 to 4.71 mmol/g, which is a decrease of only 5.42%. The CO_2 adsorption capacity for the biogas exhibits the same trend, decreasing from 4.87 to 4.59 mmol/g after ten cycles, meaning the capacity loss of only 5.75%. These capacity drops are lower than those of some amine-based adsorbents reported in the literature [49, 65]. The loss of adsorption capacity during the adsorption-desorption cycles could be due to the volatilization of the impregnated TEPA [51, 66].

4. Conclusions

Mesoporous MgO was synthesized and functionalized by impregnation with different tetraethylenepentamine (TEPA) loadings. The prepared MgO-TEPA was used as an adsorbent for CO_2 separation from simulated biogas. The CO_2 adsorption capacity of the adsorbents was found to increase with increasing TEPA loading. MgO-TEPA-40 with 40 wt.% TEPA exhibits the best CO_2 adsorption performance, with the CO_2 adsorption capacity of 4.98 mmol/g. However, a further increase in TEPA loading to 50 wt.% causes a significant reduction of CO_2 adsorption capacity. The stability

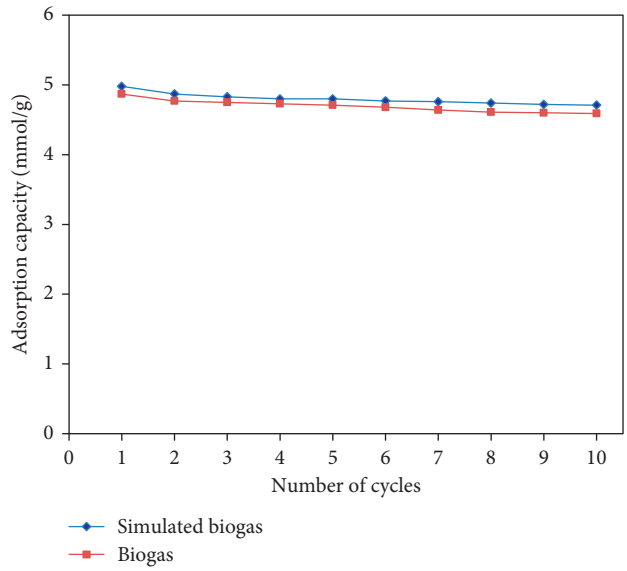

Figure 6: Cyclic CO_2 adsorption capacities of MgO-TEPA-40.

and regenerability of MgO-TEPA-40 were examined by performing ten consecutive CO_2 adsorption-desorption runs under simulated biogas and real biogas conditions. MgO-TEPA-40 shows slight decreases of only 5.42 and 5.75% of CO_2 adsorption capacity for the simulated biogas and biogas, respectively, after ten cycles. These results indicate that MgO-TEPA-40 has a stable CO_2 adsorption capacity and good regenerability both in simulated biogas and biogas, which are beneficial properties for practical applications as CO_2 adsorbent.

Data Availability

The data used to support the findings of this study are included within the article.

Conflicts of Interest

The authors declare that there are no conflicts of interest regarding the publication of this paper.

Acknowledgments

The authors gratefully acknowledge the Faculty of Science and Technology, Prince of Songkla University, for the instruments and facilities used in this study.

References

[1] M. Poeschl, S. Ward, and P. Owende, "Environmental impacts of biogas deployment-part II: life cycle assessment of multiple production and utilization pathways," *Journal of Cleaner Production*, vol. 24, pp. 184–201, 2012.

[2] W. Fan, Y. Liu, and K. Wang, "Detailed experimental study on the performance of monoethanolamine, diethanolamine, and diethylenetriamine at absorption/regeneration conditions," *Journal of Cleaner Production*, vol. 125, pp. 296–308, 2016.

[3] I. Angelidaki, L. Treu, P. Tsapekos et al., "Biogas upgrading and utilization: current status and perspectives," *Biotechnology Advances*, vol. 36, no. 2, pp. 452–466, 2018.

[4] L. Lombardi and E. Carnevale, "Economic evaluations of an innovative biogas upgrading method with CO_2 storage," *Energy*, vol. 62, pp. 88–94, 2013.

[5] S. Rasi, A. Veijanen, and J. Rintala, "Trace compounds of biogas from different biogas production plants," *Energy*, vol. 32, no. 8, pp. 1375–1380, 2007.

[6] J. Arroyo, F. Moreno, M. Muñoz, C. Monné, and N. Bernal, "Combustion behavior of a spark ignition engine fueled with synthetic gases derived from biogas," *Fuel*, vol. 117, pp. 50–58, 2014.

[7] O. W. Awe, Y. Zhao, A. Nzihou, D. P. Minh, and N. Lyczko, "A Review of biogas utilisation, purification and upgrading technologies," *Waste and Biomass Valorization*, vol. 8, no. 2, pp. 267–283, 2017.

[8] E. Ryckebosch, M. Drouillon, and H. Vervaeren, "Techniques for transformation of biogas to biomethane," *Biomass and Bioenergy*, vol. 35, no. 5, pp. 1633–1645, 2011.

[9] G. T. Rochelle, "Amine scrubbing for CO_2 capture," *Science*, vol. 325, no. 5948, pp. 1652–1654, 2009.

[10] B. Dutcher, M. Fan, and A. G. Russell, "Amine-based CO_2 capture Technology development from the beginning of 2013-A review," *ACS Applied Materials and Interfaces*, vol. 7, no. 4, pp. 2137–2148, 2015.

[11] C.-H. Yu, C.-H. Huang, and C.-S. Tan, "A review of CO_2 capture by absorption and adsorption," *Aerosol and Air Quality Research*, vol. 12, no. 5, pp. 745–769, 2012.

[12] S. Ma'mun, R. Nilsen, and H. F. Svendsen, "Solubility of carbon dioxide in 30 mass % monoethanolamine and 50 mass % methyldiethanolamine solutions," *Journal of Chemical and Engineering Data*, vol. 50, no. 2, pp. 630–634, 2005.

[13] B. P. Mandal and S. S. Bandyopadhyay, "Absorption of carbon dioxide into aqueous blends of 2-amino-2-methyl-1-propanol and monoethanolamine," *Chemical Engineering Science*, vol. 61, no. 16, pp. 5440–5447, 2006.

[14] G.-P. Hao, W.-C. Li, and A.-H. Lu, "Novel porous solids for carbon dioxide capture," *Journal of Materials Chemistry*, vol. 21, no. 18, pp. 6447–6451, 2011.

[15] R. V. Siriwardane, M.-S. Shen, E. P. Fisher, and J. A. Poston, "Adsorption of CO_2 on molecular sieves and activated carbon," *Energy and Fuels*, vol. 15, no. 2, pp. 279–284, 2001.

[16] A. E. Ogungbenro, D. V. Quang, K. Al-Ali, and M. R. M. Abu-Zahra, "Activated carbon from date seeds for CO2 capture applications," *Energy Procedia*, vol. 114, pp. 2313–2321, 2017.

[17] S. Loganathan, M. Tikmani, and A. K. Ghoshal, "Novel pore-expanded MCM-41 for CO_2 capture: synthesis and characterization," *Langmuir*, vol. 29, no. 10, pp. 3491–3499, 2013.

[18] R. V. Siriwardane, M.-S. Shen, E. P. Fisher, and J. Losch, "Adsorption of CO_2 on zeolites at moderate temperatures," *Energy and Fuels*, vol. 19, no. 3, pp. 1153–1159, 2005.

[19] M. Mofarahi and F. Gholipour, "Gas adsorption separation of CO_2/CH_4 system using zeolite 5A," *Microporous and Mesoporous Materials*, vol. 200, pp. 1–10, 2014.

[20] D. Britt, H. Furukawa, B. Wang, T. G. Glover, and O. M. Yaghi, "Highly efficient separation of carbon dioxide by a metal-organic framework replete with open metal sites," *Proceedings of National Academy of Sciences*, vol. 106, no. 49, pp. 20637–20640, 2009.

[21] A. R. Millward and O. M. Yaghi, "Metal–Organic frameworks with exceptionally high capacity for storage of carbon dioxide at room temperature," *Journal of American Chemical Society*, vol. 127, no. 51, pp. 17998-17999, 2005.

[22] N. Gargiulo, F. Pepe, and D. Caputo, "CO_2 adsorption by functionalized nanoporous materials: a review," *Journal of Nanoscience and Nanotechnology*, vol. 14, no. 2, pp. 1811–1822, 2014.

[23] G. Qi, Y. Wang, L. Estevez et al., "High efficiency nanocomposite sorbents for CO_2 capture based on amine-functionalized mesoporous capsules," *Energy and Environmental Science*, vol. 4, no. 2, pp. 444–452, 2011.

[24] H. Y. Huang, R. T. Yang, D. Chinn, and C. L. Munson, "Amine-grafted MCM-48 and silica xerogel as superior sorbents for acidic gas removal from natural gas," *Industrial and Engineering Chemistry Research*, vol. 42, no. 12, pp. 2427–2433, 2003.

[25] P. J. E. Harlick and A. Sayari, "Applications of pore-expanded mesoporous silica. 5. Triamine grafted material with exceptional CO_2 Dynamic and equilibrium adsorption performance," *Industrial and Engineering Chemistry Research*, vol. 46, no. 2, pp. 446–458, 2007.

[26] N. Hiyoshi, K. Yogo, and T. Yashima, "Adsorption characteristics of carbon dioxide on organically functionalized SBA-15," *Microporous and Mesoporous Materials*, vol. 84, no. 1–3, pp. 357–365, 2005.

[27] A. C. C. Chang, S. S. C. Chuang, M. Gray, and Y. Soong, "In-situ infrared study of CO_2 Adsorption on SBA-15 grafted with γ-(aminopropyl)triethoxysilane," *Energy and Fuels*, vol. 17, no. 2, pp. 468–473, 2003.

[28] X. Xu, C. Song, J. M. Andresen, B. G. Miller, and A. W. Scaroni, "Novel polyethylenimine-modified mesoporous molecular sieve of MCM-41 type as high-capacity adsorbent for CO_2 Capture," *Energy and Fuels*, vol. 16, no. 6, pp. 1463–1469, 2002.

[29] M. B. Yue, Y. Chun, Y. Cao, X. Dong, and J. H. Zhu, "CO_2 capture by as-prepared SBA-15 with an occluded organic template," *Advanced Functional Materials*, vol. 16, no. 13, pp. 1717–1722, 2006.

[30] M. B. Yue, L. B. Sun, Y. Cao et al., "Promoting the CO_2 adsorption in the amine-containing SBA-15 by hydroxyl group," *Microporous and Mesoporous Materials*, vol. 114, no. 1–3, pp. 74–81, 2008.

[31] R. Sanz, G. Calleja, A. Arencibia, and E. S. Sanz-Pérez, "CO_2 adsorption on branched polyethyleneimine-impregnated mesoporous silica SBA-15," *Applied Surface Science*, vol. 256, no. 17, pp. 5323–5328, 2010.

[32] K. Zhou, S. Chaemchuen, and F. Verpoort, "Alternative materials in technologies for Biogas upgrading via CO_2 capture," *Renewable and Sustainable Energy Reviews*, vol. 79, pp. 1414–1441, 2017.

[33] M. Bhagiyalakshmi, P. Hemalatha, M. Ganesh, P. M. Mei, and H. T. Jang, "A direct synthesis of mesoporous carbon supported MgO sorbent for CO_2 capture," *Fuel*, vol. 90, no. 4, pp. 1662–1667, 2011.

[34] A. Hanif, S. Dasgupta, and A. Nanoti, "Facile synthesis of high-surface-area mesoporous MgO with excellent high-temperature CO_2 adsorption potential," *Industrial and Engineering Chemistry Research*, vol. 55, no. 29, pp. 8070–8078, 2016.

[35] Y.-D. Ding, G. Song, X. Zhu, R. Chen, and Q. Liao, "Synthesizing MgO with a high specific surface for carbon dioxide adsorption," *RSC Advances*, vol. 5, no. 39, pp. 30929–30935, 2015.

[36] G. Song, Y.-D. Ding, X. Zhu, and Q. Liao, "Carbon dioxide adsorption characteristics of synthesized MgO with various porous structures achieved by varying calcination temperature," *Colloids and Surfaces A: Physicochemical and Engineering Aspects*, vol. 470, pp. 39–45, 2015.

[37] A. Kumar and J. Kumar, "On the synthesis and optical absorption studies of nano-size magnesium oxide powder," *Journal of Physics and Chemistry of Solids*, vol. 69, no. 11, pp. 2764–2772, 2008.

[38] X. Xu, C. Song, J. M. Andrésen, B. G. Miller, and A. W. Scaroni, "Preparation and characterization of novel CO_2 "molecular basket" adsorbents based on polymer-modified mesoporous molecular sieve MCM-41," *Microporous and Mesoporous Materials*, vol. 62, no. 1-2, pp. 29–45, 2003.

[39] L. Appels, J. Baeyens, J. Degrève, and R. Dewil, "Principles and potential of the anaerobic digestion of waste-activated sludge," *Progress in Energy and Combustion Science*, vol. 34, no. 6, pp. 755–781, 2008.

[40] H. Chang and Z.-X. Wu, "Experimental study on adsorption of carbon dioxide by 5A molecular sieve for helium purification of high-temperature gas-cooled reactor," *Industrial and Engineering Chemistry Research*, vol. 48, no. 9, pp. 4466–4473, 2009.

[41] W. Zhou, S. Upreti, and M. S. Whittingham, "High performance Si/MgO/graphite composite as the anode for lithium-ion batteries," *Electrochemistry Communications*, vol. 13, no. 10, pp. 1102–1104, 2011.

[42] K. K. Han, Y. Zhou, W. G. Lin, and J. H. Zhu, "One-pot synthesis of foam-like magnesia and its performance in CO_2 adsorption," *Microporous and Mesoporous Materials*, vol. 169, pp. 112–119, 2013.

[43] X. Wang, Q. Guo, J. Zhao, and L. Chen, "Mixed amine-modified MCM-41 sorbents for CO_2 capture," *International Journal of Greenhouse Gas Control*, vol. 37, pp. 90–98, 2015.

[44] K. S. W. Sing, D. H. Everett, R. A. W. Haul et al., "Reporting physisorption data for gas/solid systems with special reference to the determination of surface area and porosity (recommendations 1984)," *Pure and Applied Chemistry*, vol. 57, no. 4, pp. 603–619, 1985.

[45] S. Ahmed, A. Ramli, and S. Yusup, "CO_2 adsorption study on primary, secondary and tertiary amine functionalized Si-MCM-41," *International Journal of Greenhouse Gas Control*, vol. 51, pp. 230–238, 2016.

[46] X. Wang, X. Ma, C. Song et al., "Molecular basket sorbents polyethylenimine-SBA-15 for CO_2 capture from flue gas: characterization and sorption properties," *Microporous and Mesoporous Materials*, vol. 169, pp. 103–111, 2013.

[47] Q. Ye, J. Jiang, C. Wang, Y. Liu, H. Pan, and Y. Shi, "Adsorption of low-concentration carbon dioxide on amine-modified carbon nanotubes at ambient temperature," *Energy and Fuels*, vol. 26, no. 4, pp. 2497–2504, 2012.

[48] M. Yao, Y. Dong, X. Hu et al., "Tetraethylenepentamine-Modified silica nanotubes for low-temperature CO_2 capture," *Energy and Fuels*, vol. 27, no. 12, pp. 7673–7680, 2013.

[49] M. Irani, K. A. M. Gasem, B. Dutcher, and M. Fan, "CO_2 capture using nanoporous TiO(OH) 2/tetraethylenepentamine," *Fuel*, vol. 183, pp. 601–608, 2016.

[50] J. Jiao, J. Cao, Y. Xia, and L. Zhao, "Improvement of adsorbent materials for CO_2 capture by amine functionalized mesoporous silica with worm-hole framework structure," *Chemical Engineering Journal*, vol. 306, pp. 9–16, 2016.

[51] W. Wang, J. Xiao, X. Wei, J. Ding, X. Wang, and C. Song, "Development of a new clay supported polyethylenimine composite for CO_2 capture," *Applied Energy*, vol. 113, pp. 334–341, 2014.

[52] L. He, M. Fan, B. Dutcher et al., "Dynamic separation of ultradilute CO_2 with a nanoporous amine-based sorbent," *Chemical Engineering Journal*, vol. 189-190, pp. 13–23, 2012.

[53] X. Ma, X. Wang, and C. Song, ""Molecular basket" sorbents for separation of $CO_2$and H_2S from various gas streams," *Journal of the American Chemical Society*, vol. 131, no. 16, pp. 5777–5783, 2009.

[54] D. Wang, C. Sentorun-Shalaby, X. Ma, and C. Song, "High-capacity and low-cost carbon-based "molecular basket" sorbent for CO2Capture from flue gas," *Energy and Fuels*, vol. 25, no. 1, pp. 456–458, 2011.

[55] W.-J. Son, J.-S. Choi, and W.-S. Ahn, "Adsorptive removal of carbon dioxide using polyethyleneimine-loaded mesoporous silica materials," *Microporous and Mesoporous Materials*, vol. 113, no. 1–3, pp. 31–40, 2008.

[56] R. Kishor and A. K. Ghoshal, "High molecular weight polyethyleneimine functionalized three dimensional mesoporous silica for regenerable CO2 separation," *Chemical Engineering Journal*, vol. 300, pp. 236–244, 2016.

[57] M. B. Yue, L. B. Sun, Y. Cao, Y. Wang, Z. J. Wang, and J. H. Zhu, "Efficient CO_2 capturer derived from as-synthesized MCM-41 modified with amine," *Chemistry-A European Journal*, vol. 14, no. 11, pp. 3442–3451, 2008.

[58] C. Chen, W.-J. Son, K.-S. You, J.-W. Ahn, and W.-S. Ahn, "Carbon dioxide capture using amine-impregnated HMS having textural Mesoporosity," *Chemical Engineering Journal*, vol. 161, no. 1-2, pp. 46–52, 2010.

[59] M. G. Plaza, C. Pevida, A. Arenillas, F. Rubiera, and J. J. Pis, "CO_2 capture by adsorption with nitrogen enriched carbons," *Fuel*, vol. 86, no. 14, pp. 2204–2212, 2007.

[60] M. G. Plaza, C. Pevida, B. Arias et al., "Application of thermogravimetric analysis to the evaluation of aminated solid sorbents for CO_2 capture," *Journal of Thermal Analysis and Calorimetry*, vol. 92, no. 2, pp. 601–606, 2008.

[61] D. V. Quang, T. A. Hatton, and M. R. M. Abu-Zahra, "Thermally stable Amine-grafted adsorbent prepared by impregnating 3-aminopropyltriethoxysilane on mesoporous silica for CO2 capture," *Industrial and Engineering Chemistry Research*, vol. 55, no. 29, pp. 7842–7852, 2016.

[62] M. L. Gray, J. S. Hoffman, D. C. Hreha et al., "Parametric study of solid amine sorbents for the capture of carbon dioxide†," *Energy and Fuels*, vol. 23, no. 10, pp. 4840–4844, 2009.

[63] J. Wang, M. Wang, B. Zhao, W. Qiao, D. Long, and L. Ling, "Mesoporous carbon-supported solid amine sorbents for low-temperature carbon dioxide capture," *Industrial and Engineering Chemistry Research*, vol. 52, no. 15, pp. 5437–5444, 2013.

[64] L. Zhang, N. Zhan, Q. Jin, H. Liu, and J. Hu, "Impregnation of polyethylenimine in mesoporous multilamellar silica vesicles for CO_2 capture: a kinetic study," *Industrial and Engineering Chemistry Research*, vol. 55, no. 20, pp. 5885–5891, 2016.

[65] L. Guo, J. Yang, G. Hu, X. Hu, H. DaCosta, and M. Fan, "CO_2 removal from flue gas with amine-impregnated titanate nanotubes," *Nano Energy*, vol. 25, pp. 1–8, 2016.

[66] Y. Wang, T. Du, Y. Song, S. Che, X. Fang, and L. Zhou, "Amine-functionalized mesoporous ZSM-5 zeolite adsorbents for carbon dioxide capture," *Solid State Sciences*, vol. 73, pp. 27–35, 2017.